



Alternating copolymers of diketopyrrolopyrrole or benzothiadiazole and alkoxy-substituted oligothiophenes: spectroscopic, electrochemical and spectroelectrochemical investigations



M. Gora^a, W. Krzywiec^b, J. Mieczkowski^a, E.C. Rodrigues Maia^{c,d}, G. Louarn^{c,*},
M. Zagorska^{b,*}, A. Pron^{b,*}

^a Faculty of Chemistry, University of Warsaw, Pasteura 1, 02-093 Warsaw, Poland

^b Faculty of Chemistry, Warsaw University of Technology, Noakowskiego 3, 00-664 Warsaw, Poland

^c Université de Nantes, CNRS, Inst. Mat. Jean Rouxel IMN, 2 rue de la Houssinière, F-44322 Nantes, France

^d Depto. de Química, Universidade Estadual de Londrina, 86057-970 Londrina, PR, Brazil

ARTICLE INFO

Article history:

Received 26 June 2014

Received in revised form 25 July 2014

Accepted 27 July 2014

Available online 13 August 2014

Keywords:

organic semiconductors
diketopyrrolopyrrole-oligothiophene
copolymers
benzothiadiazole-oligothiophene
copolymers
UV-vis-NIR spectroelectrochemistry
Raman spectroelectrochemistry vibrational
model

ABSTRACT

A series of solution processable semiconducting donor-acceptor (DA) copolymers consisting of either diketopyrrolopyrrole or benzothiadiazole A units and alkoxy- or alkyl-substituted oligothiophene D units were synthesized. For all prepared copolymers the measured XPS spectra (C1s, S2p, N1s and O1s) were in a very good agreement with the expected chemical constitution. Spectroscopic studies of the synthesized copolymers showed that their optical band gaps were governed by the presence of the alkoxy substituents whose electron donating properties led to additional gap narrowing yielding semiconductors with band gaps of below 1.3 eV in the case of the polymers with the diketopyrrolopyrrole A unit. The same trend was observed with the electrochemical band gaps, whose values were however found to be ca. 0.4 eV superior to the corresponding optical band gaps values. Vibrational model was calculated for two of the synthesized copolymers with the goal to unequivocally attribute the observed Raman modes and to support the interpretation of the spectral changes induced by the electrochemical oxidation. It was established that the electrochemical oxidative doping of the copolymer with the benzothiadiazole A unit is limited to the oligothiophene segment in which the charge of the formed polycation is localized. To the contrary, in the case of the polymer with the diketopyrrolopyrrole A segment the charge imposed on the oligothiophene segment delocalizes towards the diketopyrrolopyrrole unit. These findings are in perfect agreement with the UV-vis-NIR spectroelectrochemistry data which show strong localization of electrochemically created charge carriers in the benzothiadiazole - oligothiophene copolymer and their metallic-like delocalization in the diketopyrrolopyrrole one. The latter seems to be very interesting not only as a potential low band gap component of organic photovoltaic cells but also, in the doped state, as electronic conductor of metallic character.

© 2014 Elsevier Ltd. All rights reserved.

1. Introduction

Alternating donor-acceptor (DA) conjugated copolymers play an important role in the development of organic electronics [1–3]. They are also interesting from the point of view of applied electrochemistry since they exhibit electrochromic and electrofluorochromic effects [4]. Vivid interest in this family of electroactive materials is caused by the fact that their redox, electronic and optoelectronic properties as well as their capability of being solution

processed can be controllably tuned and adapted to a given application through the design of appropriate D and A building blocks.

Benzothiadiazoles and diketopyrrolopyrroles constitute popular electron accepting units in DA copolymers, especially with non-functionalized or functionalized oligothiophene D units [3]. Many of these polymers were tested as active components of such devices as field effect transistors (FETs) [5–11], photovoltaic cells (PC) [1,2,6,7,12–15], light emitting diodes [16,17], and others.

Copolymers of oligothiophenes and benzothiadiazoles or diketopyrrolopyrroles are electrochemically active both in oxidative and reductive regimes since the presence of an electron accepting center in the polymer repeating unit increases its electron affinity ($|EA|$) and diminishes the electrochemical gap [3]. This

* Corresponding authors.

E-mail address: zagorska@ch.pw.edu.pl (M. Zagorska).

effect is also reflected in the value of the optical band gap which makes some of these polymers interesting, solution processable near infrared absorbers [14,18,19]. Moreover, a pronounced electrochromic effect, associated with the oxidation or reduction of the neutral polymers, is observed, which involves different spectral regions than those reported for the large majority of conjugated polymers [3].

In this paper we present a joint experimental - theoretical study on a series of new diketopyrrolopyrrole (or benzothiadiazole)-oligothiophene copolymers in which the electron donating effect of the oligothiophene unit is amplified by the presence of alkoxy substituents. The obtained electrochemical and spectroelectrochemical (UV-vis-NIR and Raman) results are supported by the calculation of the vibrational models for the studied copolymers.

To clearly identify the effect of alkoxy substituents on the optical and redox properties of the alternating copolymers studied, a copolymer with alkyl substituents is also studied for comparative reasons.

2. Experimental

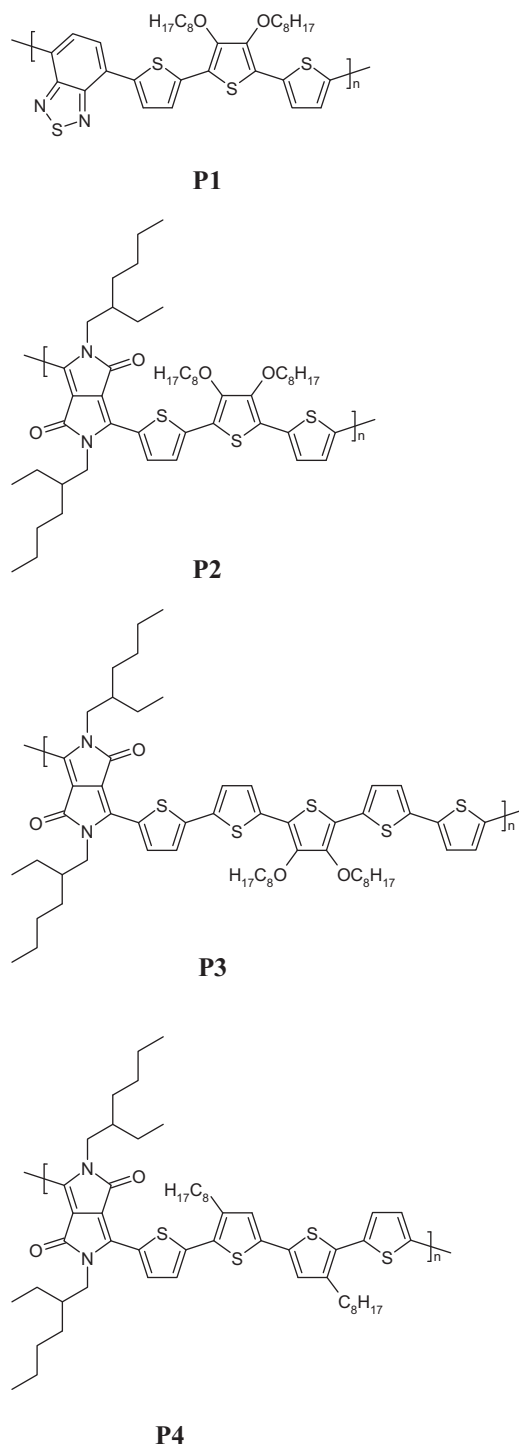
2.1. Synthesis

The investigated alternating copolymers are depicted in Scheme 1. Polymer **P1** was obtained from 5,5''-dibromo-3',4'-dioctyloxy-2,2':5',2''-terthiophene and 2,1,3-benzothiadiazole-4,7-bis(boronic acid pinacol ester) through Suzuki coupling. The remaining three copolymers were synthesized using the direct arylation method. In particular, polymer **P2** and polymer **P3** were prepared from 3,6-bis(thiophen-2-yl)-2,5-bis(2-ethylhexyl)pyrrolo[3,4-c]pyrrole-1,4(2H,5H)-dione and 2,5-dibromo-3,4-dioctyloxythiophene or 5,5''-dibromo-3',4'-dioctyloxy-2,2':5',2''-terthiophene, respectively. In the preparation of polymer **P4** the bromination of the substrates was inverted *i.e.* dibromo derivative of 3,6-bis(5-bromothiophen-2-yl)-2,5-bis(2-ethylhexyl)pyrrolo[3,4-c]pyrrole-1,4(2H,5H)-dione was reacted with 4,4'-dioctyl-2,2'-bithiophene. All four polymers were precipitated with methanol, then repeatedly washed with this solvent and finally dried. **P1** was additionally washed with acetone to remove the shortest oligomers as recommended in [20]. Its macromolecular parameters were as follows; $M_w = 3499$ Da, $PDI = 4.7$. Sequential fractionation of **P3** and **P4** with CH_2Cl_2 and $CHCl_3$ yielded two fractions. In both cases more abundant CH_2Cl_2 fraction was taken for further investigations (for **P3** $M_w = 4432$ Da, $PDI = 2.8$; for **P4** $M_w = 5609$ Da, $PDI = 2.4$). **P2** could not be fractionated in this manner and as prepared polymer after washing with methanol and drying showed $M_w = 5275$ Da, $PDI = 4.61$. Molecular weight was determined by size exclusion chromatography (SEC) in CH_2Cl_2 . The detailed description of the synthetic procedures for monomers and polymers can be found in *Supplementary data*.

2.2. X-ray photoelectron spectroscopy

XPS measurements were performed with an Axis Nova instrument from Kratos Analytical spectrometer with Al $K\alpha$ line (1486.6 eV) as an excitation source. Survey spectra were acquired at pass energies of 80 eV. The core level spectra (C 1s, O 1s, N 1s and S 2p) were acquired with an energy step of 0.1 eV and using a constant pass energy mode of 20 eV, to obtain data in a reasonable experimental time (energy resolution of 0.48 eV). The pressure in the analysis chamber was maintained lower than 10^{-7} Pa.

Data analysis was carried out using CasaXPS software. In the used approach, the background spectra are considered as



Scheme 1. Chemical formulae of the investigated DA alternating copolymers.

Shirley-type and curve fitting is accomplished with a mixture of Gaussian-Lorentzian functions. Concerning the calibration, binding energy for the C1s hydrocarbons peak was set at 284.8 eV. The error in defining the position of peaks is estimated at about 0.1 eV. No surface cleaning, using Ar sputtering for example was applied. It is known that carbonaceous atmospheric contamination on the sample's surface usually occurs, but taking into account the soft matter nature of the polymers studied, ion sputtering can be suspected of changing the chemical composition and inducing structural damage.

2.3. Raman scattering and infrared absorption spectroscopy

Raman spectra of neutral and oxidized copolymers were recorded on a R enishaw InVia reflex spectrometer ($\lambda_{\text{exc}} = 514.5$ nm, laser power = 10 mW, 2 μm diameter spot, typical exposure times 60 sec) or on a FT Raman Bruker RFS 100 spectrometer with the near-IR excitation line (1064 nm, laser power = 50 mW). Fourier transform infrared spectroscopy (FTIR) was recorded on a Bruker Vertex 70 spectrometer (4 cm^{-1}).

2.4. UV-vis-NIR spectroscopy

Solution spectra of **P1** - **P4** dissolved in chloroform and solid state spectra of their thin layers were recorded using a Varian Cary 5000 spectrometer. Thin layers of polymers were deposited on a quartz substrate by drop-casting.

2.5. Cyclic voltammetry, UV-vis-NIR and Raman spectroelectrochemistry

For the cyclic voltammetry studies thin layers of polymers **P1**–**P4** were deposited on a platinum electrode. The measurement were carried out in a three electrode cell in a dry argon atmosphere on an Autolab potentiostat (Eco Chimie). The electrolytic medium consisted of a 0.1 M solution of Bu_4NBF_4 in acetonitrile. A platinum counter electrode, and a $\text{Ag}/0.1\text{ M AgNO}_3/\text{CH}_3\text{CN}$ reference electrode were used. The potential of the reference electrode with respect to the ferrocene redox couple was always measured after each experiment. The same working electrode, cell and electrolyte were used for Raman spectroelectrochemistry. For UV-vis-NIR spectroelectrochemical measurement thin layers of polymers were deposited on an ITO electrode, the rest of the electrochemical equipment remaining the same. Spectroelectrochemical experiments were carried out in the oxidative mode. The potential of the working electrode was being increased in small increments. After each potential raise, a wait time was applied until the quasi-equilibrium state was reached, then the UV-vis-NIR or Raman spectrum was registered. It was assumed that the equilibrium state was reached when the potential change induced current became negligible.

2.6. Computational methods

Quantum chemical calculations were limited to **P1** and **P3** as representative examples of two types of DA polymers studied. Density functional theory calculations were performed with Gaussian 09 [21] at the B3LYP level of theory and employing the 6-31 + G(d,p) basis set for the macromolecules structure optimization. The geometry optimization resulted in a nonplanar geometry, and no imaginary frequencies were observed in the calculated spectrum. However, to interpret more precisely the vibrational spectra and their experimental evolutions as a function of the oxidation potential, normal coordinate calculations were carried out using general valence force field. This calculations method has previously been successfully applied to other conjugated polymers [22] and polymers consisting of alternating conjugated and non-conjugated segments [23]. The used methodology is described in detail in [24]. It can be briefly summarized as follows. The calculations of the force field and frequencies are carried out using the Fourier's dynamic matrix. Since the macromolecules of **P1** and **P3** possess translational symmetry, the calculations can be restricted to one repeat unit. They require the knowledge of force constants, bond lengths, and bond angles. An internal coordinate system is used to compute the fundamental vibrations of the studied copolymers. The local redundancies can be handled by suitable symmetry coordinates. The calculation starts from a minimal set of force

Table 1
Optical parameters of the studied copolymers (**P1**–**P4**).

polymer	solution $\lambda_{\text{max}}/\text{nm}$	thin film $\lambda_{\text{max}}/\text{nm}$	thin film $\lambda_{\text{onset}}/\text{nm}$	E_g optical/eV
P1	407, 595	415, 628	833	1.49
P2	390, 751	416, 755	1000	1.23
P3	432, 686	445 (shoulder), 692	908	1.37
P4	309, 654	432, 690	892	1.39

constants expressed in terms of internal coordinates. It is necessary to assume that certain force constants must be fairly local *i.e.* depending on the position and the type of a few nearest neighbours. For this reason they can be transferred from other compounds of appropriate chemical structure. Hence, force constants corresponding to common groups were expected to be transferable among these molecules. The number of force constants utilized in the calculations has to be minimized. This approach leads to a significant reduction of the number of independent parameters, which becomes much lower than the number of observed frequencies.

The final parameters are adjusted from experimental and calculated frequencies using a least-squares root procedure. The vibrational normal-mode assignments were based on the best-fit comparison of the calculated Raman spectrum with the observed FT-Raman spectrum, after adjusting the calculated wavenumbers. In these conditions the refinement yielded an average error of 7 cm^{-1} between the observed and calculated frequencies.

3. Results and discussion

The main effect of the donor-acceptor interactions in alternating DA copolymers is narrowing of the band gap, through re-hybridization of bonds. This effect is manifested by a significant bathochromic shift of their $\pi - \pi^*$ transitions towards lower energies (bathochromic shift) as compared to those recorded for the corresponding homopolymers [25]. Being low band gap semiconductors, these copolymers are very well suited for the fabrication of organic photovoltaic cells or ambipolar transistors [3].

UV-vis spectra registered for chloroform solution and thin films of all polymers studied are shown in Fig. 1, whereas the corresponding spectroscopic data, together with the optical gap values, are collected in Table 1. In the solution spectrum of **P1** two clear absorption bands can be distinguished at 407 nm and at 595 nm which undergo a bathochromic shift in the solid state spectrum to 415 nm and 628 nm, respectively. In similar polymers both bands bathochromically shift with increasing strength of the donor [25]. The position of the lower energetic band in **P1** clearly manifests the electron donating effect of the alkoxy substituents since in the spectra of benzothiadiazole-based copolymers in which the D segments consist of either unsubstituted or alkyl-substituted thiophene rings, this band appears in the 530 nm - 560 nm range [26–28]. It is found at higher wavelengths than in the case of **P1** only in DA copolymers where the rotation of the adjacent thiophene rings in the D segment is blocked by an appropriate bridging group [29] or the D unit consists of fused heterocyclic rings [30–33].

Copolymers of diketopyrrolopyrrole with oligothiophenes also exhibit two bands in their UV-vis spectra: a very weak band in the vicinity of 400 - 450 nm and a strong one of lower energy whose position is dependent on the nature of the donor segment [34]. In the spectra of polymers in which the D unit consists of alkyl substituted oligothiophene this band is located at shorter wavelengths than in alkoxy-substituted **P3** [34]. If fused aromatic groups are used as donor segments such as thienoacenes [35] or pyrroloindacenodithiophene [36] than this band is bathochromically shifted as compared to the corresponding band in the spectrum of **P3**.

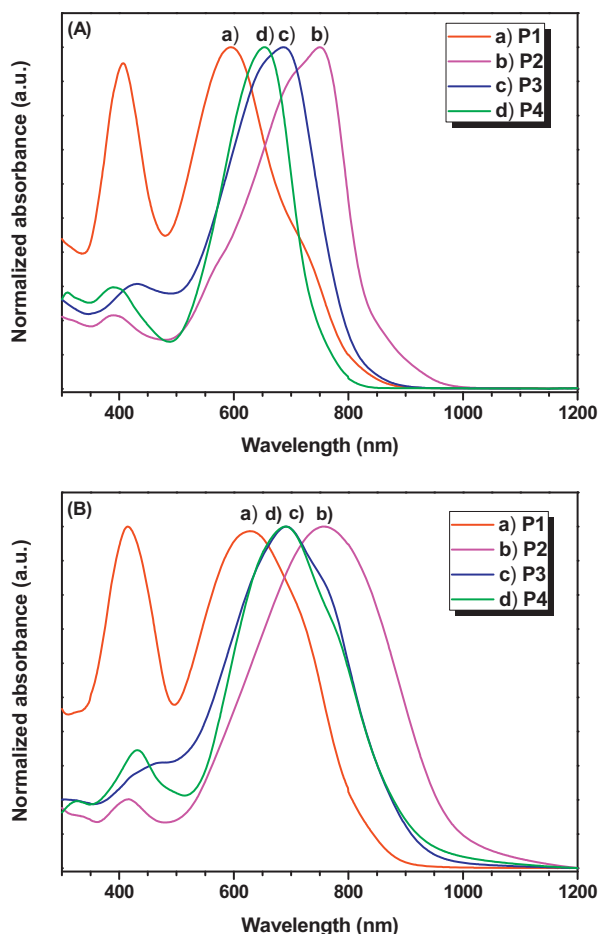


Fig. 1. Normalized UV-vis absorption spectra of copolymers for solutions in CHCl_3 (A) and for thin solid layers (B).

A comparison of **P1** and **P2** is instructive. Since in both polymers the D units are identical, the observed difference in the $\pi - \pi^*$ bands position must originate from more pronounced electron accepting character of diketopyrrolopyrrole which results in stronger DA interactions in **P2**. The effect of electron donating alkoxy substituents is, in turn, clearly evidenced by comparing the spectrum of **P2** with that of **P3**. Shortening of the oligothiophene segment from five rings in **P3** to three rings in **P2**, while keeping the central ring with two alkoxy substituents unchanged, results in an additional bathochromic shift of the $\pi - \pi^*$ band and further band gap narrowing. In **P4**, which contains alkyl substituents in the oligothiophene segment, the $\pi - \pi^*$ transition is more energetic in solution spectra than in the case of **P2** and **P3** giving rise to a clear band at shorter wavelengths, again consistent with weaker DA interactions.

The XPS spectra of **P1** and **P3** are shown in Fig. 2 as representative examples whereas all XPS data are collected in Table 2. For all copolymers the surficial elemental composition, as measured by XPS, is in good agreement with expected structures. In addition, only residual quantities of bromine arising from the substrates can be detected. However, it should be stressed that under the applied

Table 2
Atomic percentages of C, N, O, S and Br measured for thin films of **P1** - **P4**.

polymer	C (%)	N (%)	O (%)	S (%)	Br (%)
P1	83.7	3.3	5.1	7.0	0.9
P2	83.8	2.8	10.0	3.4	< 0.1
P3	84.1	2.5	9.2	4.1	< 0.1
P4	88.1	2.5	4.9	4.2	0.2

work conditions, the accuracy is surprisingly good. A small excess of oxygen, with respect to the stoichiometries of the studied polymers, consistently found for all samples, probably originates from the fact that no surface cleaning by Ar sputtering was applied (see Experimental part).

The following most striking features of the XPS spectra should be noted: (i) a shift of the signals corresponding to N(1s) from 399.4 eV in **P1** (C=N-C) to 399.9 eV in **P3** (C-N-C); (ii) two clearly identifiable S(2p_{1/2}) peaks in the spectrum of **P1** at 163.8 eV and 164.8 eV, ascribed to thiophene and benzothiadiazole sulfur, respectively; (iii) the O(1s) peak in the spectrum of **P1** (C-O-C of alkoxy groups), at 532.7 eV splitted into two components in the corresponding spectrum of **P3**, at 532.7 and 530.8 eV, the latter being consistent with the presence of the keto groups; (iv) a small atomic percentage of bromine (< 0.9 ± 0.2%) is recorded, originating from chain end groups, but this contribution is minor, especially for **P2** and **P3**. Finally, it should be noticed the C(1s) signal can be deconvoluted into two or three main lines, indicating the presence of at least 3 types of carbon bonds: sp² carbons in the conjugated core and sp³ carbons in the substituents (~ 284.8 eV), C-S (thiophene, thiadiazole), C-N (thiadiazole), C-O-C (alkoxy groups) (286.0 eV) and C=O (diketopyrrolopyrrole) (>287 eV).

Cyclic voltammetry is a convenient research tool for studying the effect of the nature of A and D segments in a given alternating copolymer on its redox properties. In Fig. 3a and b cyclic voltammograms of thin layers of **P1** and **P3**, deposited on a platinum electrode by casting from a chloroform solution, are compared, whereas those of **P2** and **P4** can be found in Fig. S1 of Supplementary information. In the oxidative doping mode **P1** yields two strongly overlapping anodic peaks at 0.28 V and 0.54 V vs Fc/Fc⁺, which have even broader cathodic counterparts. This part of the cyclic voltammogram strongly resembles that of an alternating copolymer of 3,4-dialkoxythiophene and 2,2'-bithiophene [37], whose repeating unit is the same as the D unit in **P2**. A small shift of the two anodic peaks towards higher potentials is caused by the presence of benzothiadiazole acceptors in the polymer main chain. In the negative potentials range a reversible redox couple is observed corresponding to the reduction of the neutral polymer chain to a polyanion and its consecutive oxidation to the neutral state upon the scan reversal.

In the oxidative mode, the electrochemical behavior of **P3** resembles that of **P1**, its reduction at negative potentials is however only partially reversible and the cathodic peak has two overlapping anodic counterparts (Fig. 3b). The voltammogram of **P4** in both anodic and cathodic parts is similar to that registered for **P3**, however, the oxidation peak is shifted towards higher potentials. This can be considered as a manifestation of weaker electron donating properties of alkyl substituents as compared to alkoxy ones. The electrochemical parameters of **P1**-**P4**, together with their electrochemically determined ionization potentials (IPs) and electron affinities (EAs) as well as electrochemical band gaps, are listed in Table 3.

It should be stated here that the listed-IP and EA values, determined from cyclic voltammetry experiments, are the same as the values termed as "electrochemically determined HOMO and LUMO levels". We prefer-IP and EA instead of HOMO and LUMO levels since the latter are not experimental observables but the results of quantum chemical calculations, although their values being closely related to-IP and EA. Moreover, electrochemical IP values very well correlate with IPs determined by UPS which is a direct method of this parameter determination [38].

To summarize this part of the research, the obtained cyclic voltammetry results are consistent with the UV-vis ones, showing in addition that the potentials of the oxidative doping in the studied copolymers (and by consequence their ionization potentials (IP)) are governed mainly by the nature of the solubilizing substituents

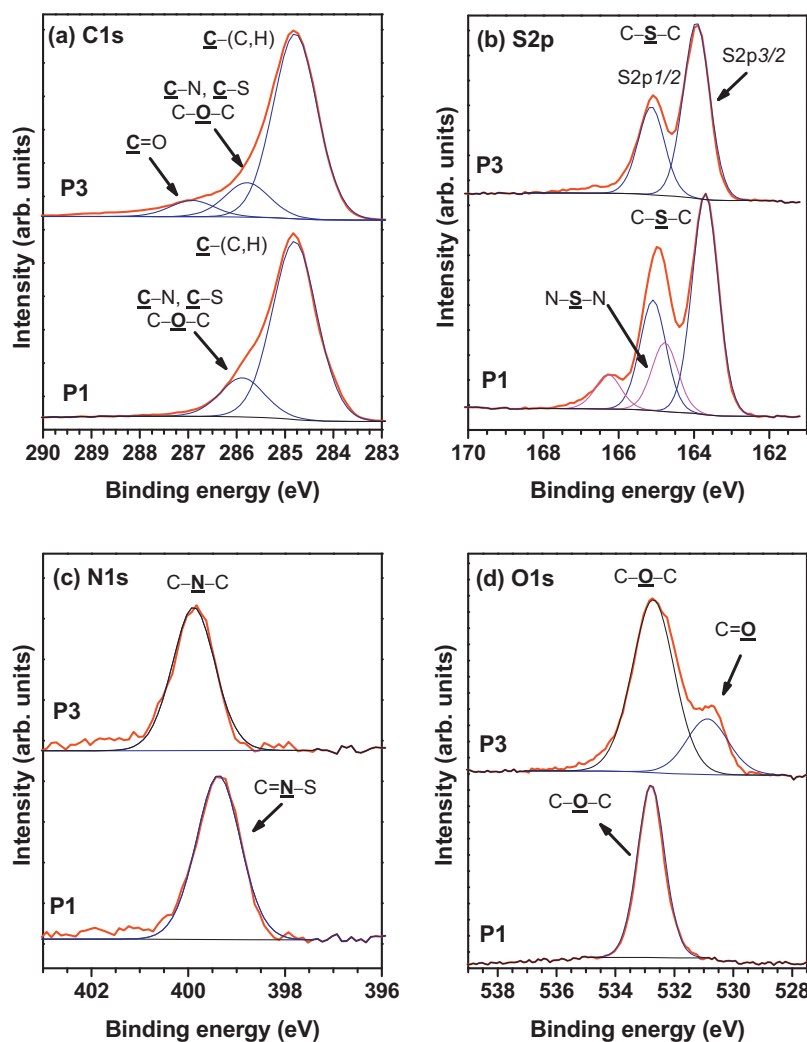


Fig. 2. XPS spectra of **P1** and **P3**: a) C1s, b) S2p, c) N1s and d) O1s core level spectra and curve-fitting results.

in the oligothiophene segment and to a lesser extent by the nature of the acceptor group. The latter determines, in turn, their potential of the reductive doping and the electron affinity (EA).

In the UV-vis-NIR spectroelectrochemical investigations of electroactive conjugated polymers two types of spectral evolution are typically found. In the first type, oxidation of a neutral polymer chain to a polycation, advancing with increasing working electrode potential, results in bleaching of the absorption band characteristic of the $\pi - \pi^*$ transition with concomitant growth of two oxidation-induced bands ascribed to specific charge storage configurations, namely localized bipolarons and polarons. These two bands persist after the complete $\pi - \pi^*$ band bleaching. In the second type of spectroelectrochemical response, at potentials corresponding to the complete or nearly complete bleaching of the $\pi - \pi^*$ band, the two oxidation-induced bands merge, yielding “an absorption tail” showing monotonically increasing absorbance

with increasing wavelength. This absorption tail is attributed to delocalized bipolarons and is characteristic of the metallic state [39]. By electron-hole symmetry, the same spectroelectrochemical behaviour is found in the process of electrochemical reduction of the neutral conjugated polymers to polyanions (reductive or n-type doping). The doping-induced bands correspond in this case to either localized or delocalized negative bipolarons and polarons [40].

In Fig. 4a UV-vis-NIR spectra of **P1**, registered for increasing working electrode potentials, are presented. The obtained spectroelectrochemical data are in line with the voltammetric ones. The first oxidation induced spectral changes appear at $E = 0.06$ V vs Fc/Fc^+ i.e. at a potential which is only 50 mV lower than the potential of the oxidation onset in the cyclic voltammogram. This small shift of the oxidative doping onset, as probed by the UV-vis-NIR spectroelectrochemistry, can be rationalized by the fact that

Table 3

Electrochemical parameters of the studied copolymers (**P1 - P4**). Potentials given vs Fc/Fc^+ .

polymer	E_{red1}/V	E_{ox1}/V	$E_{red1(onset)}/V$	E_{ox2}/V	E_{red2}/V	$E_{ox2(onset)}/V$	EA*/eV	IP*/eV	E_g electrochem/eV
P1	-1.76	-1.62	-1.67	0.28, 0.54	0.17	0.11	-3.43	5.21	1.78
P2	-1.56	-1.47	-1.45	0.52	0.42	0.25	-3.65	5.35	1.70
P3	-1.62	-1.53–1.32	-1.52	0.34	0.31	0.20	-3.58	5.30	1.72
P4	-1.69	-1.57	-1.52	0.5	0.47	0.21	-3.58	5.31	1.73

*Calculated using the following equations: EA(eV) = $-|e|(E_{red1(onset)} + 5.1)$, IP(eV) = $|e|(E_{ox2(onset)} + 5.1)$

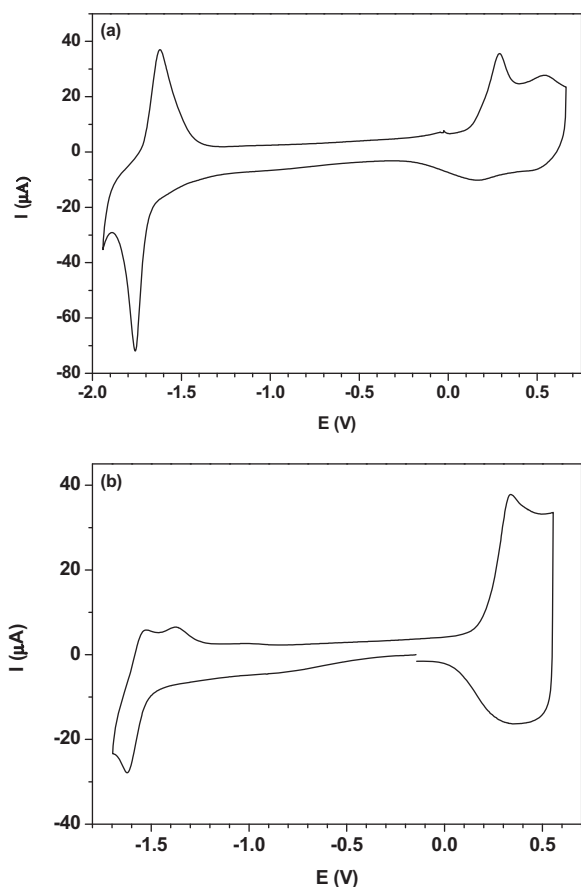


Fig. 3. Cyclic voltammogram of **P1** (a) and **P3** (b). Electrolyte 0.1 M Bu_4NBF_4 in acetonitrile, scan rate 50 mV/s, E vs Fc/Fc^+ .

the measurements presented here were performed in a *quasi*-static mode: the electrode potential was raised in small increments and after each potential raise a wait time was applied until the equilibrium state was reached in which the measured current dropped to zero or to a negligible value. The UV-vis-NIR spectrum was registered after this wait time. This technique tends to detect the first signs of oxidative doping at slightly lower potentials than cyclic voltammetry which is dynamic in nature. At the end of the oxidation ($E = 0.56 \text{ V}$) two doping-induced broad bands at 790 nm and 1770 nm dominate the spectrum. This means that the formed charge storage configurations (positive bipolarons and polarons) are localized and the metallic state has not been reached. Similar spectroelectrochemical behaviour was found for an alternating copolymer of benzothiadiazole and unsubstituted bithiophene [26]. There exist however reports on “metallic-like” UV-vis-NIR spectra of fully doped alternating copolymers of alkoxy-substituted bithiophenes and benzothiadiazole [41] as well as copolymers of dithienopyrroles and benzothiadiazole [31].

Spectral response of **P3** to the working electrode potential increase is shown in Fig. 4b. Again, the obtained results are fully consistent with the voltammetric data. Similarly as in the case of **P1**, oxidation-induced spectral changes start at a slightly lower potential (0.15 vs Fc/Fc^+), than the onset of the anodic peak in the cyclic voltammogram. One should notice that at the highest potential, corresponding to the end of the anodic peak, the recorded spectrum is nearly “metallic” in character.

The change of the appearance of the polymer films during their UV-vis-NIR spectroelectrochemical investigation is shown in Fig. 4c. The oxidation of **P1** induces a variation of its color from greenish to blue. The concomitant increase of the film transparency

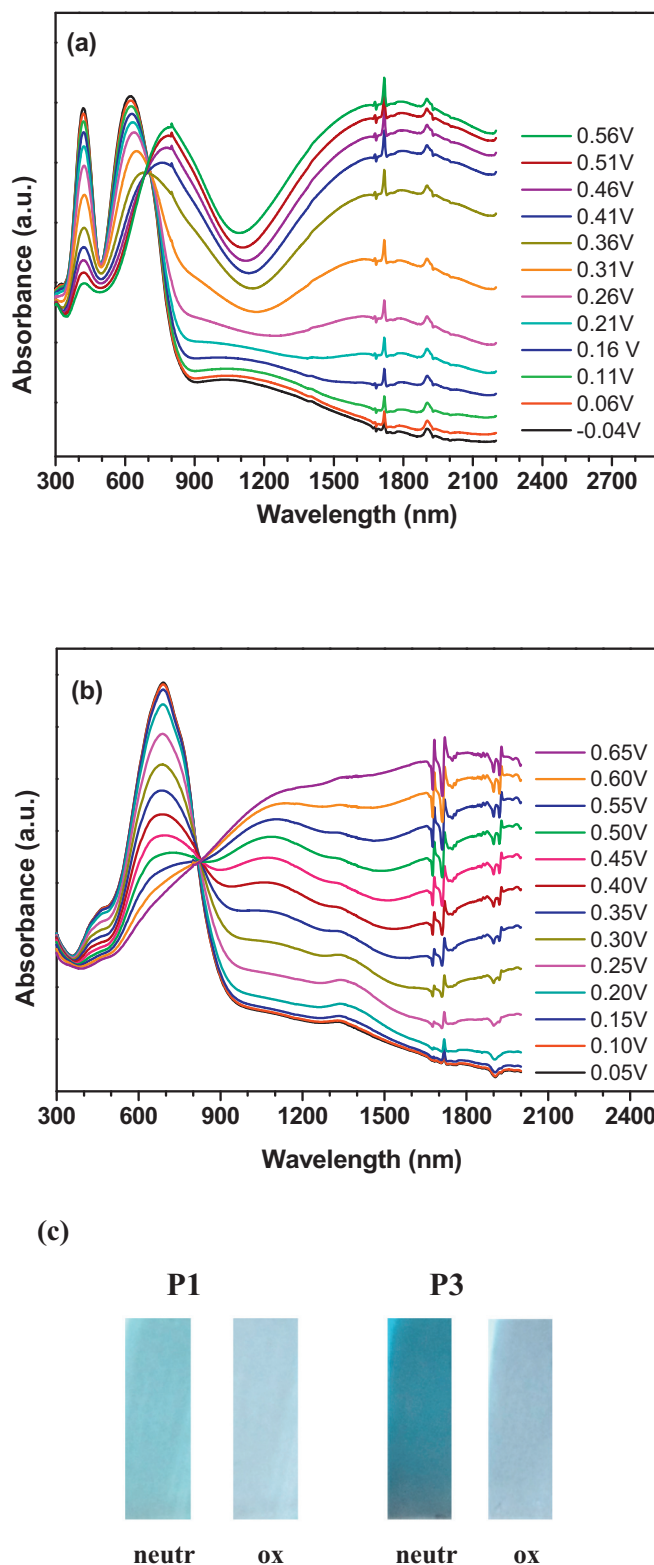


Fig. 4. Evolution of the UV-vis-NIR spectra with increasing working electrode potential: (a) **P1** (b) **P3**. Electrolyte 0.1 M Bu_4NBF_4 in acetonitrile, E vs Fc/Fc^+ . (c) Images of colored neutral and oxidized films of **P1** and **P3**.

is a result of bleaching of both absorption bands (415 and 628 nm) present in the visible part of the neutral polymer spectrum. Similar features are observed for **P3**, which changes the color from dark blue, characteristic of neutral low band gap polymers, to highly transparent light blue.

Raman spectroelectrochemistry is also a very powerful tool for studying the redox properties of conjugated polymers. The oxidation of these polymers chain to polycations (or reduction to polyanions) affects the force constants of selected bonds and frequently induces changes in the chain geometry. As a result profound doping-induced changes in the Raman spectra are observed which involve disappearance or shifts of some bands and appearance of new ones. One should also be aware of the fact that in Raman spectroelectrochemical studies of conjugated polymers resonance effects are frequently observed and the resulting spectra strongly depend on the position of the excitation wavelength with respect to the observed electronic transitions. Moreover, since the oxidation or reduction processes profoundly change the UV-vis-NIR spectra of these compounds the resonance conditions change with increasing (decreasing) working electrode potential [23,42]. All these factors must be taken into consideration in any spectroelectrochemical study.

In Fig. 5 Raman and IR spectra of all four copolymers studied are presented. To facilitate the attribution of bands and to better elucidate structural changes induced by the oxidative doping we have established vibrational models for **P1** and **P3**. In developing these models we have optimized the macromolecules geometries using DFT calculations. The obtained bond lengths as well as angles between bonds and the obtained force constants (FG matrix) are shown in Chart S1 and S2 of *Supplementary Information*. The experimentally measured and calculated vibrational modes are listed in Table 4, where their attribution is additionally given (for more complete description of Raman scattering and infrared absorption bands of the studied copolymers see *Supplementary Information*).

Vibrational attributions listed in Table 4 were done with the support of previous publications and exploiting the potential energy distributions (PED) [44,45]. Results presented in these tables are largely self-explanatory, so the discussion is limited to the evolution of the modes during the spectroelectrochemical experiments. In addition, it should be stressed here that infrared absorption data were mainly dominated by bands from alkyl group. So, assignments of infrared absorption bands was not fully performed.

Fig. 6 shows the evolution of the Raman spectra of **P1** with increasing working electrode potential. The observed spectral changes start at $E=0.10$ V vs. Fc/Fc^+ , fairly consistent with the UV-vis-NIR spectroelectrochemical data. The most pronounced changes can be described as follows. In poly(thiophene) homopolymers with alkoxy substituents two bands in the spectral range of 1420 – 1480 cm^{-1} dominate the spectrum. They are ascribed to $\text{C}_\alpha\text{-C}_\beta$ stretchings in the nonsubstituted and alkoxy-substituted thiophene rings [37,46]. These bands can be found in the spectrum of neutral **P1** at 1428 cm^{-1} and 1471 cm^{-1} . Upon electrochemical oxidation they shift to lower wave numbers. In particular, at $E=0.6$ V the former is located at 1417 cm^{-1} , whereas the second merges with the residual 1428 cm^{-1} band and is present as a shoulder. The band at 1368 cm^{-1} , originating from $\text{C}_\beta\text{-C}_\beta$ of the thiophene ring shifts towards higher wavenumbers (1378 cm^{-1}) upon the electrochemical oxidation [47]. Concomitantly the band at 1205 cm^{-1} , ascribed to $\text{C}_\alpha\text{-C}_\alpha$ interring stretchings in the oligothiophene segment increases in intensity. These changes are very similar to those observed in poly(thiophene) homopolymers containing alkoxy substituents [37,46]. Thus, Raman spectroelectrochemical results seem to indicate that the oxidation of **P1** takes place on the donor units whose benzoid-type structure is being transformed into the quinoid one as in the case of poly(thiophene) homopolymers. Since the UV-vis-NIR spectra show that the formed bipolarons are localized, it may be concluded that the benzothiadiazole units constitute obstacles against the delocalization of these charge storage configurations. To confirm this assumption, we can stress here that the main characteristic Raman bands of

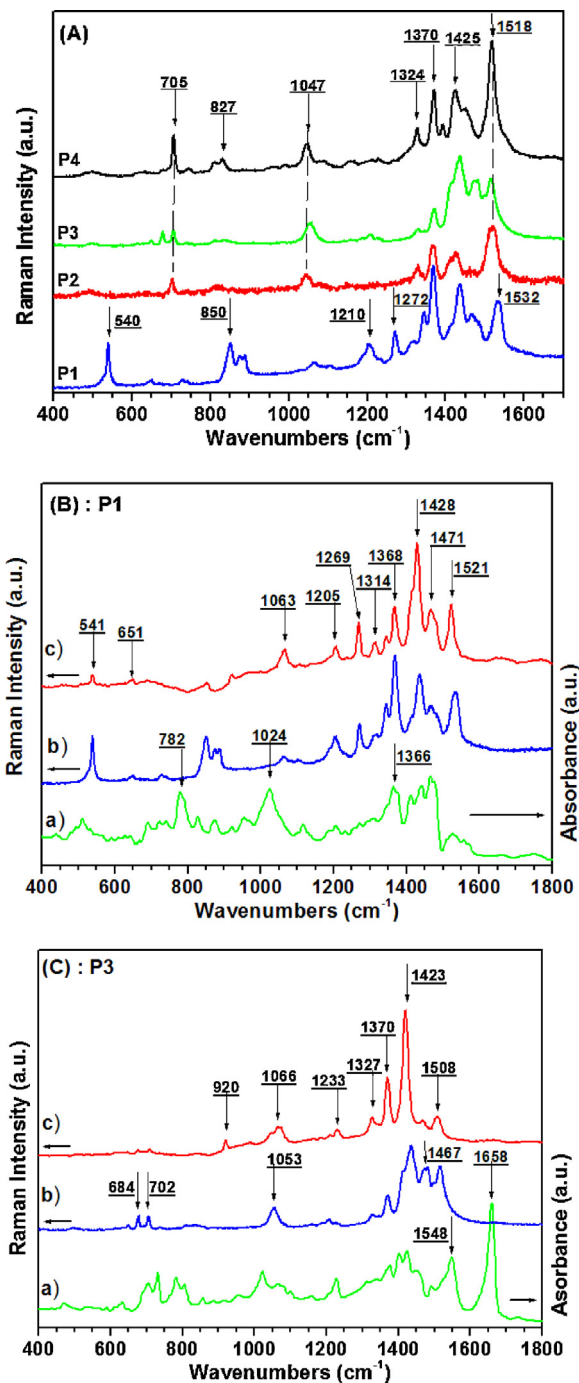


Fig. 5. Vibrational spectra of the studied copolymers: (A) Raman spectra (514.5 nm) of **P1**–**P4**; (B) Raman scattering and infrared absorption of **P1**; a) FTIR spectrum, b) and c) Raman scattering (514.5 and 1064 nm excitation wavelength respectively); (C) Raman scattering and infrared absorption of **P3**; a) FTIR spectrum, b) and c) Raman scattering (514.5 and 1064 nm excitation wavelength respectively).

the benzothiadiazole moieties, the C–C stretch of benzothiadiazole aromatic ring observed at $1521/1532\text{ cm}^{-1}$ and 1269 cm^{-1} , are unaffected by the electrochemical oxidation.

Raman spectroelectrochemical response of **P3** is shown in Fig. 7. Up to $E=0.2$ V vs. Fc/Fc^+ , apart from lowering of the peaks intensity no change in their positions can be noticed. This means that only non oxidized segments give rise to Raman bands, being however progressively more and more out of resonance. No bands characteristic of the oxidized (doped) form can be detected. Above this

Table 4
Calculated and experimentally measured frequencies (in cm^{-1}) of the main vibrational modes of **P1** and **P3** in their neutral form. Vibrational modes of regioregular poly(3-hexylthiophene), P3HT, reported in [43] are given for comparison.

P1		P3		PTh/P3HT	Assignments
Exptl bands	Calcd modes	Exptl bands	Calcd modes	ν/cm^{-1}	
3062 ⁽¹⁾	3063	3065 ⁽¹⁾	3063	3072	C–H stretch (thiophene ring)
2950 ⁽¹⁾	-	2950 ⁽¹⁾	-	2950	
2920 ⁽¹⁾	-	2920 ⁽¹⁾	-	2920	methyl symmetric CH stretching
2850 ⁽¹⁾	-	2850 ⁽¹⁾	-	2850	methylene antisymmetric CH stretching
		1658 ⁽¹⁾	1655		methylene antisymmetric CH stretching
		1548 ⁽¹⁾	1541		C=O stretch (DPP group)
		1508	1521		C=C asym stretch (DPP group)
1521	1530				C=C sym stretch (DPP group)
1471	1465	1467	1465	1515	C–C aromatic stretch (BTD group)
1428	1430	1423	1430	1438	C=C asym stretch (thiophene group)
1368	1370	1370	1370	1385	C=C sym stretch (thiophene group)
		1327	1331		C–C stretch (thiophene group)
1314	1320				C–C stretch (DPP group)
1269	1270				C=N stretch + C=N–S def (BTD group)
1205	1225	1233	1225	1208	C–C stretch (benzothiadiazole aromatic ring)
		1066	1065		C–C inter-ring stretch
1063	1045	1053	1045	1045	C–N stretch + ring deformation (DPP group)
1023 ⁽¹⁾	1021	1023 ⁽¹⁾	1021	1015	C–H bend (thiophene ring)
887	899				C–O–C deformation (alkoxythiophene group)
875	883				N–S–N + ring deformation (BTD group)
854	860				
		827	812		C–H out-of-plane bend (BTD group)
730	728				DPP and thiophene ring in-plane deformation
		705	716	724	In-plane ring deformation of the BTD group
		684	696		C–S–C stretch + ring defm (thiophene ring)
541	551				in-plane ring deformation of the BTD group

⁽¹⁾ from infrared absorption spectra; BTD - benzothiadiazole; DPP - diketopyrrolopyrrole

potential the spectrum gains features characteristic of the oxidized state. At $E = 0.6\text{ V}$ vs. Fc/Fc^+ all bands corresponding to $\text{C}_{\alpha}\text{--}\text{C}_{\beta}$ symmetric (1420 cm^{-1}) and asymmetric stretchings (1467 cm^{-1}) of the thiophene ring undergo a shift to lower wave numbers— 1403 and $\sim 1439\text{ cm}^{-1}$ (shoulder), respectively. The band at 1371 cm^{-1} which is ascribed to $\text{C}_{\beta}\text{--}\text{C}_{\beta}$ stretching in the thiophene ring, in the oxidized sample is located at slightly higher wave numbers (1374 cm^{-1}). Finally the band attributed to $\text{C}_{\alpha}\text{--}\text{C}_{\alpha}$ interring stretchings grows in intensity with increasing working electrode potential. All these changes unequivocally prove the oxidation of the oligothiophene segments. The next question to be answered is whether the modes characteristic of diketopyrrolopyrrole (DPP) moiety are affected by the chain oxidation or they remain unchanged as in the case of benzothiadiazole (BTD) modes? The band at 1508 cm^{-1} , assigned to the C=C stretching mode in the DPP moiety shifts to 1478 cm^{-1} whereas the position of the C–C stretching band

at 1327 cm^{-1} remains essentially unchanged with the electrode potential increase. This observation indicates that the π -system of DPP is affected by the oxidation of the oligothiophene segment and the positive charge imposed on the chain during electrochemical oxidation can delocalize through the conjugated pathway of the DPP moiety. The obtained results are fully consistent with the UV-vis-NIR spectroelectrochemical data which clearly indicate charge carriers delocalization in **P3** (see Fig. 4). Additional support for this conclusion comes from DFT calculations which indicate planarity of the thienylene-DPP-thienylene segment in **P3** whereas in the corresponding thienylene-BTD-thienylene segment of **P1** a torsion angle of 27° is found. Thus, Raman spectroelectrochemical data clearly show that BTD units in **P1** constitute an obstacle for charge carriers delocalization whereas in **P3** this delocalization passes through the DPP units. For the reader's convenience all oxidation induced changes in Raman modes of **P1** and **P3** are listed in Table 5.

Table 5
Raman frequencies (in cm^{-1}) of the main vibrational modes of **P1** and **P3** in their neutral and highest oxidation state. Potentials given versus Fc/Fc^+ .

P1		P3		Assignments
Exptl bands		Exptl bands		
Neutral (-0.2 V)	Oxidized (0.6 V)	Neutral (-0.2 V)	Oxidized (0.6 V)	
		1508	1478	C=C sym stretch (DPP group)
1521	1516			C–C aromatic stretch (BTD group)
1471	shoulder	1467	shoulder	C=C asym stretch (thiophene group)
1428	1417	1420	1403	C=C asym stretch (thiophene group)
1368	1367	1370	1374	C–C stretch (thiophene group)
1314	1339			C=N stretch + C=N–S def. (BTD group)
		1327	1326	C–C stretch (DPP group)
1269	1262			C–C stretch (benzothiadiazole aromatic ring)
1205	1204	1233	1210	C–C inter-ring stretch
1063	1105	1066	1093	C–H def. (semi-quinonoid thiophene ring)

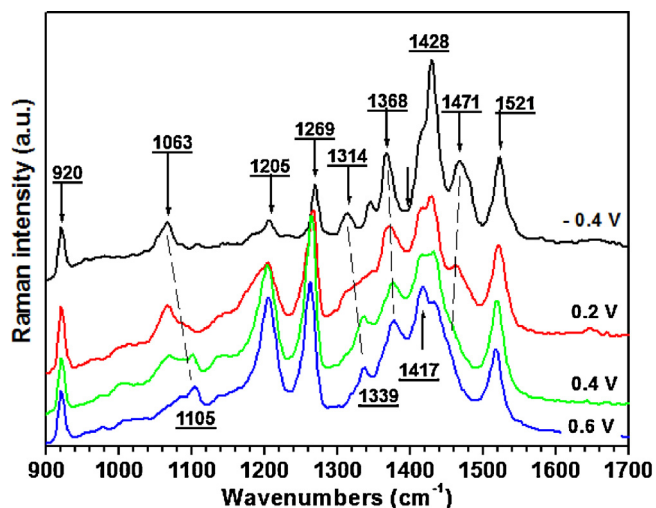


Fig. 6. Raman spectra ($\lambda_{\text{exc}} = 1064 \text{ nm}$) of P1 recorded at increasing working electrode potentials. Electrolyte 0.1 M Bu₄NBF₄ in acetonitrile, E vs Fc/Fc⁺.

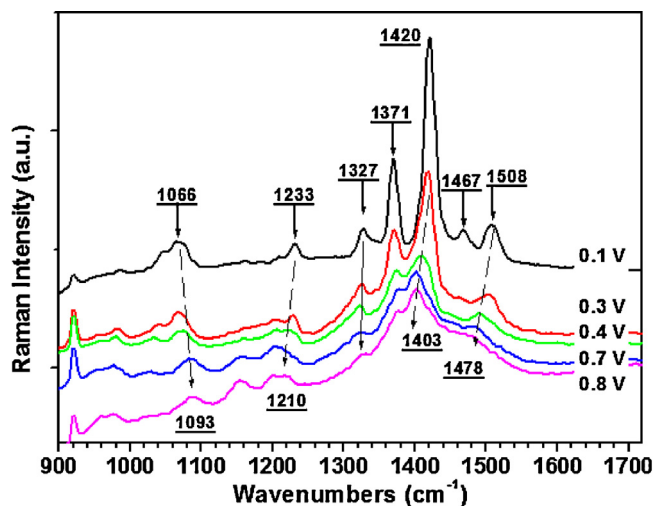


Fig. 7. Raman spectra ($\lambda_{\text{exc}} = 1064 \text{ nm}$) of P3 recorded at increasing working electrode potentials. Electrolyte 0.1 M Bu₄NBF₄ in acetonitrile, E vs Fc/Fc⁺.

4. Conclusions

To summarize, we have synthesized new donor-acceptor (DA) alternating copolymers consisting of either diketopyrrolopyrrole or benzothiadiazole A units and oligothiophenes disubstituted with alkoxy groups in the central ring as D units. Complementary spectroscopic, electrochemical and spectroelectrochemical investigations have shown that the widths of the optical and electrochemical band gaps in these copolymers are governed by the presence of the alkoxy substituents whose electron donating properties lead to additional gap narrowing. Copolymers with diketopyrrolopyrrole A units show significantly lower band gaps than their benzothiadiazole analogues containing the same D unit. UV-vis-NIR and Raman spectroelectrochemical investigations clearly indicate that the charge imposed on the polymer chain during electrochemical oxidation to radical cation is delocalized in the case of P3 (the copolymer with the diketopyrrolopyrrole acceptor unit) and localized to oligothiophene segments in the case of P1 (the benzothiadiazole - oligothiophene copolymer). Therefore, the former seems to be very interesting not only as a potential low band gap component of organic photovoltaic cells but also, in the doped state, as electronic conductor of metallic character.

Acknowledgment

This work has been supported in part by the European Union in the framework of Regional Development Fund through the Joint UW and WUT International PhD Program of Foundation for Polish Science—“Towards Advanced Functional Materials and Novel Devices” (MPD/2010/4). W.K. and A.P. acknowledge the financial support of Foundation for the Polish Science Team Programme co-financed by the EU European Regional Development “New solution processable organic and hybrid (organic/inorganic) functional materials for electronics, optoelectronics and spintronics” (Contract No. TEAM/2011-8/6). M.G. thanks for financial support from National Science Centre (Poland) through a research project PRELUDIUM 5, 2013/09/N/ST5/02987.

Appendix A. Supplementary data

Supplementary data associated with this article can be found, in the online version, at <http://dx.doi.org/10.1016/j.electacta.2014.07.147>.

References

- [1] Y.-J. Cheng, S.-H. Yang, C.-S. Hsu, Synthesis of conjugated polymers for organic solar cell applications, *Chem. Rev.* 109 (2009) 5868–5923.
- [2] A.J. Heeger, Semiconducting polymers: the third generation, *Chem. Soc. Rev.* 39 (2010) 2354–2371.
- [3] P. Bujak, I. Kulszewicz-Bajer, M. Zagorska, V. Maurel, I. Wielgus, A. Pron, Polymers for electronics and spintronics, *Chem. Soc. Rev.* 42 (2013) 8895–8999.
- [4] Kim, J., Do, E., Kim, G., Clavier, L., Galmiche, P., Audebert, Tetrazine-based electrochromic windows: Modulation of the fluorescence through applied potential, *J. Electroanal. Chem.* 632 (2009) 201–205.
- [5] C.B. Nielsen, M. Turbiez, I. McCulloch, Recent advances in the development of semiconducting DPP-containing polymers for transistor applications, *Adv. Mater.* 25 (2013) 1859–1880.
- [6] Y. Li, P. Sonar, L. Murphy, W. Hong, High mobility diketopyrrolopyrrole (DPP)-based organic semiconductor materials for organic thin film transistors and photovoltaics, *Energy Environ. Sci.* 6 (2013) 1684–1710.
- [7] M.A. Naik, S. Patil, Diketopyrrolopyrrole-based conjugated polymers and small molecules for organic ambipolar transistors and solar cells, *J. Polym. Sci. Part A: Polym. Chem.* 51 (2013) 4241–4260.
- [8] H. Bronstein, Z. Chen, R.S. Ashraf, W. Zhang, J. Du, J.R. Durrant, P.S. Tuladhar, K. Song, S.E. Watkins, Y. Geerts, M.M. Wienk, R.A.J. Janssen, T. Anthopoulos, H. Sirringhaus, M. Heeney, I. McCulloch, Thieno[3,2-b]thiophene-diketopyrrolopyrrole-containing polymers for high-performance organic field-effect transistors and organic photovoltaic devices, *J. Am. Chem. Soc.* 133 (2011) 3272–3275.
- [9] P. Sonar, S.P. Singh, Y. Li, M.S. Soh, A. Dodabalapur, A low-bandgap diketopyrrolopyrrole-benzothiadiazole-based copolymer for high-mobility ambipolar organic thin-film transistors, *Adv. Mater.* 22 (2010) 5409–5413.
- [10] Z. Chen, M.J. Lee, R.S. Ashraf, Y. Gu, S. Albert-Seifried, M.M. Nielsen, B. Schroeder, T.D. Anthopoulos, M. Heeney, I. McCulloch, H. Sirringhaus, High-performance ambipolar diketopyrrolopyrrole-thieno[3,2-b]thiophene copolymer field-effect transistors with balanced hole and electron mobilities, *Adv. Mater.* 24 (2012) 647–652.
- [11] H.N. Tsao, D.M. Cho, I. Park, M.R. Hansen, A. Mavrinskiy, D.Y. Yoon, R. Graf, W. Pisula, H.W. Spiess, K. Mullen, Ultrahigh mobility in polymer field-effect transistors by design, *J. Am. Chem. Soc.* 133 (2011) 2605–2612.
- [12] S. Qu, H. Tian, Diketopyrrolopyrrole (DPP)-based materials for organic photovoltaics, *Chem. Commun.* 48 (2012) 3039–3051.
- [13] L. Huo, J. Hou, H. -Yu Chen, S. Zhang, Y. Jiang, T.L. Chen, Y. Yang, Bandgap and molecular control of the low-bandgap polymers based on 3,6-dithiophen-2-yl-2,5-dihydropyrrolo[3,4-c]pyrrole-1,4-dione toward highly efficient polymer solar cells, *Macromolecules* 42 (2009) 6564–6571.
- [14] E. Zhou, S. Yamakawa, K. Tajima, C. Yang, K. Hashimoto, Synthesis and photovoltaic properties of diketopyrrolopyrrole-based donor-acceptor copolymers, *Chem. Mater.* 21 (2009) 4055–4061.
- [15] M. Wang, X. Hu, P. Liu, W. Li, X. Gong, F. Huang, Y. Cao, Donor-acceptor conjugated polymer based on naphtho[1,2-c:5,6-c']bis[1,2,5]thiadiazole for high-performance polymer solar cells, *J. Am. Chem. Soc.* 133 (2011) 9638–9641.
- [16] Z. Qiao, Y. Xua, S. Lina, J. Peng, D. Cao, Synthesis and characterization of red-emitting diketopyrrolopyrrole-alt-phenylenevinylene polymers, *Synth. Met.* 160 (2010) 1544–1550.
- [17] D. Kabra, L.P. Lu, M.H. Song, H.J. Snaith, R.H. Friend, Efficient single-layer polymer light-emitting diodes, *Adv. Mater.* 22 (2010) 3194–3198.
- [18] D. Deng, L. Gu, Synthesis and photovoltaic properties of new near infrared absorption polymers based on C and N-bridged dithiophene and diketopyrrolopyrrole units, *J. Mater. Sci.: Mater. Electron.* 24 (2013) 3029–3035.

- [19] Q. Guo, J. Dong, D. Wan, D. Wu, J. You, Modular establishment of a diketopyrrolopyrrole - based polymer library via Pd-catalyzed direct C-H (hetero)arylation: a highly efficient approach to discover low-bandgap polymers, *Macromol. Rapid Commun.* 34 (2013) 522–527.
- [20] M. Trznadel, A. Pron, M. Zagorska, R. Chrzaszcz, J. Pieliowski, Effect of molecular weight on spectroscopic and spectroelectrochemical properties of regioregular poly(3-hexylthiophene), *Macromolecules* 31 (1998) 5051–5058.
- [21] M. J. Frisch, G. W. Trucks, H. B. Schlegel, G. E. Scuseria, M. A. Robb, J. R. Cheeseman, G. Scalmani, V. Barone, B. Mennucci, G. A. Petersson, H. Nakatsuji, M., Caricato, X., Li, H. P. Hratchian, A. F. Izmaylov, J., Bloino, G., Zheng, J. L. Sonnenberg, M., Hada, M., Ehara, K., Toyota, R., Fukuda, J., Hasegawa, M., Ishida, T., Nakajima, Y., Honda, O., Kitao, H., Nakai, T., Vreven, J. A. Montgomery, Jr., J. E. Peralta, F., Ogliaro, M., Bearpark, J. J. Heyd, E., Brothers, K. N. Kudin, V. N. Staroverov, R., Kobayashi, J., Normand, K., Raghavachari, A., Rendell, J. C. Burant, S. S. Iyengar, J., Tomasi, M., Cossi, N., Rega, J. M. Millam, M., Klene, J. E. Knox, J. B. Cross, V., Bakken, C., Adamo, J., Jaramillo, R., Gomperts, R. E. Stratmann, O., Yazyev, A. J. Austin, R., Cammi, C., Pomelli, J. W. Ochterski, R. L. Martin, K., Morokuma, V. G. Zakrzewski, G. A. Voth, P., Salvador, J. J. Dannenberg, S., Dapprich, A. D. Daniels, O., Farkas, J. B. Foresman, J. V. Ortiz, J. Cioslowski, and D. J. Fox, Gaussian 09, Revision A.02, Gaussian, Inc., Wallingford CT, 2009.
- [22] M. Cochet, G. Louarn, S. Quillard, M.I. Boyer, J.-P. Buisson, S. Lefrant, Theoretical and experimental study of polyaniline in base forms: non-planar analysis. Part I, *J. Raman Spectrosc.* 31 (2000) 1029–1039.
- [23] P. Gawrys, G. Louarn, M. Zagorska, A. Pron, Solid state electrochemistry and spectroelectrochemistry of poly(arylene bisimide-alt-oligoether)s, *Electrochim. Acta* 56 (2011) 3429–3435.
- [24] G. Louarn, M. Lapkowski, S. Quillard, A. Pron, S. Lefrant, Vibrational properties of polyaniline: isotope effects, *J. Phys. Chem.* 100 (1996) 6998–7006.
- [25] P.M. Beaujuge, S. Ellinger, J.R. Reynolds, The donor-acceptor approach allows a black-to-transmissive switching polymeric electrochrome, *Nature Materials* 7 (2008) 795–799.
- [26] O. Atwani, C. Baristiran, A. Erden, G. Sonmez, A stable, low band gap electroactive polymer: Poly(4,7-dithien-2-yl-2,1,3-benzothiadiazole), *Synth. Met.* 158 (2008) 83–89.
- [27] J. Hou, H.-Y. Chen, S. Zhang, Y. Yang, Synthesis and photovoltaic properties of two benzo[1,2-*b*:3,4-*b'*]dithiophene-based conjugated polymers, *J. Phys. Chem. C* 113 (2009) 21202–21207.
- [28] L. Biniek, C.L. Chochos, N. Leclerc, G. Hadziioannou, J.K. Kallitsis, R. Bechara, P. Lévêque, T. Heiser, A. [3,2-*b*]thienothiophene-alt-benzothiadiazole copolymer for photovoltaic applications: design, synthesis, material characterization and device performances, *J. Mater. Chem.* 19 (2009) 4946–4951.
- [29] D. Mühlbacher, M. Scharber, M. Morana, Z. Zhu, D. Waller, R. Gaudiana, C. Brabec, High photovoltaic performance of a low-bandgap polymer, *Adv. Mater.* 18 (2006) 2884–2889.
- [30] H.-H. Chang, C.-E. Tsai, Y.-Y. Lai, D.-Y. Chiou, S.-L. Hsu, C.-S. Hsu, Y.-J. Cheng, Synthesis, molecular and photovoltaic properties of donor - acceptor conjugated polymers incorporating a new heptacyclic indacenodithieno[3,2-*b*]thiophene arene, *Macromolecules* 45 (2012) 9282–9291.
- [31] X. Zhang, T.T. Steckler, R.R. Dasari, S. Ohira, W.J. Potscavage Jr., S.P. Tiwari, S. Coppée, S. Ellinger, S. Barlow, J.-L. Bredas, B. Kippelen, J.R. Reynolds, S.R. Marder, Dithienopyrrole-based donor-acceptor copolymers: low band-gap materials for charge transport, photovoltaics and electrochromism, *J. Mater. Chem.* 20 (2010) 123–134.
- [32] V. Tamilavan, M. Song, R. Agneeswari, J.-W. Kang, D.-H. Hwang, M.H. Hyun, Synthesis and photovoltaic properties of donor acceptor polymers incorporating a structurally-novel pyrrole-based imide-functionalized electron acceptor moiety, *Polymer* 54 (2013) 6150–6157.
- [33] A.K. Palai, A. Kumar, K. Shashidhara, S.P. Mishra, Polyalkylthiophene-containing electron donor and acceptor heteroaromatic bicycles: synthesis, photophysical, and electroluminescent properties, *J. Mater. Sci.* 49 (2014) 2456–2464.
- [34] M.M. Wienk, M. Turbiez, J. Gilot, R.A.J. Janssen, Narrow-bandgap diketopyrrolo-pyrrole polymer solar cells: the effect of processing on the performance, *Adv. Mater.* 20 (2008) 2556–2560.
- [35] Z. Zeng, Y. Li, J. Deng, Q. Huang, Q. Peng, Synthesis and photovoltaic performance of lowband gap copolymers based on diketopyrrolopyrrole and tetrathienoacene with different conjugated bridges, *J. Mater. Chem. A* 2 (2014) 653–662.
- [36] J.E. Donaghey, E.-H. Sohn, R.S. Ashraf, T.D. Anthopoulos, S.E. Watkins, K. Song, C.K. Williams, I. McCulloch, Pyrroloindacenodithiophene polymers: the effect of molecular structure on OFET performance, *Polym. Chem.* 4 (2013) 3537–3544.
- [37] R. Pokrop, I. Kasprzyk-Mlynarczyk, M. Zagorska, I. Wielgus, J. Mieczkowski, J.M. Verilhac, J. Wery, Alternate copolymer of 3,4-dioctyloxythiophene and 2,2'-bithiophene: Synthesis, electronic and spectroelectrochemical properties, *Polish. J. Chem.* 81 (2007) 731–744.
- [38] R. Rybakiewicz, P. Gawrys, D. Tsikritzis, K. Emmanouil, S. Kennou, M. Zagorska, A. Pron, Electronic properties of semiconducting naphthalene bisimide, derivatives—Ultraviolet photoelectron spectroscopy versus electrochemistry, *Electrochim. Acta* 96 (2013) 13–17.
- [39] T.-C. Chung, J.H. Kaufman, A.J. Heeger, F. Wudl, Charge storage in doped poly(thiophene): Optical and electrochemical studies, *Phys. Rev. B* 30 (1984) 702–710.
- [40] K. Kotwica, E. Kurach, G. Louarn, A.S. Kostyuchenko, A.S. Fisyuk, M. Zagorska, A. Proń, Alternating copolymers of thiadiazole and quaterthiophenes—Synthesis, electrochemical and spectroelectrochemical characterization, *Electrochim. Acta* 111 (2013) 491–498.
- [41] P.M. Beaujuge, S.V. Vasilyeva, S. Ellinger, T.D. McCarley, J.R. Reynolds, Unsaturated linkages in dioxythiophene-benzothiadiazole donor-acceptor electrochromic polymers: the key role of conformational freedom, *Macromolecules* 42 (2009) 3694–3706.
- [42] R. Demadrille, M. Zagorska, M. Billon, G. Louarn, S. Lefrant, A. Pron, Solution versus solid state electropolymerization of regioregular conjugated fluorenone-thienylene vinylene macromonomers—voltammetric and spectroelectrochemical investigations, *J. Solid State Electrochem* 11 (2007) 1051–1058.
- [43] G. Louarn, M. Trznadel, J.-P. Buisson, J. Laska, A. Pron, M. Lapkowski, S. Lefrant, Raman spectroscopic studies of regioregular poly(3-alkylthiophenes), *J. Phys. Chem.* 100 (1996) 12532–12539.
- [44] F.R. Dollish, W.G. Fateley, F.F. Bentley, Characteristic Raman frequencies of organic compounds, Wiley, 1974.
- [45] S. Quillard, G. Louarn, S. Lefrant, A.G. MacDiarmid, Vibrational analysis of Polyaniline: a comparative study of leucoemeraldine, emeraldine, and pernigraniline bases, *Phys. Rev. B* 50 (1994) 12496–12508.
- [46] A. Pron, G., Louarn, M., Lapkowski, M., Zagorska, J. Glowczyk-Zubek, S. Lefrant, in situ Raman spectroelectrochemical studies of poly(3,3'-dibutoxy-2,2'-bithiophene), *Macromolecules* 28 (1995) 4644–4649.
- [47] G. Louarn, J.P. Buisson, S. Lefrant, D. Fichou, Vibrational studies of a series of α -oligothiophenes as model systems of polythiophene, *J. Phys. Chem.* 99 (1995) 11399–11404.